Alone in a crowd: Effect of a nonfunctional lateral line on expression of the social hormone *parathyroid hormone 2*.

Alexandra Venuto[1], Cameron P. Smith[1,2], Marybelle Cameron-Pack[3], and Timothy Erickson[3]

1. East Carolina University, Greenville, NC, USA
2. East Carolina University School of Dental Medicine, Greenville, NC, USA
3. University of New Brunswick, Fredericton, NB, CAN

Corresponding author: Timothy Erickson, timothy.erickson@unb.ca

Key words: hair cells, lateral line, neuropeptide, pth2, social brain, zebrafish

SUMMARY STATEMENT

Expression of the pro-social neuropeptide *pth2* is downregulated in larval zebrafish with a congenital loss of lateral line function. Thus, even in social environments, fish with compromised lateral lines may experience a form of isolation.

ABSTRACT

Parathyroid hormone 2 (Pth2) is a vertebrate-specific neuropeptide whose thalamic expression is upregulated by social contact with conspecifics. However, social interactions fail to stimulate *pth2* expression in isolated zebrafish whose lateral line hair cells have been chemically ablated. These results suggest that modulation of *pth2* by social context is acutely dependent on mechanosensory information from the lateral line. However, it is unclear how a congenital loss of lateral line function influences the ability of zebrafish to interpret their social environment. In this study, we measure *pth2* levels in zebrafish mutants lacking hair cell function in either the lateral line only, or in both the inner ear and lateral line. Socially-raised lateral line mutants express lower levels of *pth2* relative to wild type siblings, but there is no further reduction when all sensory hair cells are nonfunctional. However, social isolation of hair cell mutants causes a further reduction in *pth2* expression, pointing to additional unidentified sensory cues that influence *pth2* production. Lastly, we report that social context modulates fluorescent transgenes driven by the *pth2* promoter. Altogether, these data suggest that lateral line mutants experience a form of isolation, even when raised in a social environment.

INTRODUCTION

The complex relationship between the brain and social behavior has been studied across animal species for decades (Brothers, 1990; Chen and Hong, 2018; Kravitz and Huber, 2003; Robinson et al., 2008). Different social contexts can evoke a wide range of emotions, from joy and positivity (Burgdorf and Panksepp, 2006; Panksepp and Burgdorf, 2003) to fear and aggression (Amaral, 2002; Neumann et al., 2010) with a high level of plasticity (Chen and Hong, 2018; Kolb and Whishaw, 2003). In situations of social isolation, many animals exhibit anxious behaviors in addition to neurochemical changes in the brain (Amaral, 2002; Mumtaz et al., 2018; Shams et al., 2017; Weiss et al., 2004).

Social behavior is modulated by a suite of neuropeptides (Adkins-Regan, 2009; O'Connell and Hofmann, 2011; Oldfield and Hofmann, 2011; Panksepp et al., 2007; Schoofs et al., 2017). Parathyroid hormone 2 (Pth2, formerly known as tuberoinfundibular peptide of 39 residues or TIP39) is a neuropeptide expressed in the vertebrate thalamus, which is a sensory integration and relay center (Anneser et al., 2020; Bhattacharya et al., 2011; Dobolyi et al., 2012; Mueller, 2012). In rodents, the PTH2 receptor is expressed in several nuclei throughout the central nervous system (Dobolyi et al., 2012). Zebrafish have two *pth2r* paralogs, *pth2ra* and *pth2rb,* each with distinct expression patterns in the fish brain (Seitz, 2019). Activation of PTH2R increases intracellular cAMP levels and can modulate neuroendocrine activity in the hypothalamic–pituitary–adrenal (HPA) axis (Dimitrov and Usdin, 2010). PTH2-PTH2R signaling influences several behaviors, including maternal care (Cservenák et al., 2013), pain sensitivity (Dimitrov et al., 2010; Dimitrov et al., 2013; LaBuda and Usdin, 2004), and anxiety-like responses (Anneser et al., 2022; Coutellier and Usdin, 2011; LaBuda et al., 2004).

Recent work suggests that Pth2 signaling promotes social interactions between conspecifics. In zebrafish, *pth2* mutants exhibit decreased preference for conspecifics (Anneser et al., 2022), while chemogenetic activation of the Pth2-positive region of the rodent brain promotes social contact (Keller et al., 2022). Consistent with this, expression of *pth2* itself positively scales with the quantity of social interactions with conspecifics (Anneser et al., 2020; Anneser et al., 2022; Keller et al., 2022). In rodents, physical touch from conspecifics activates *Pth2* expression (Cservenák et al., 2013; Keller et al., 2022). In addition to tactile touch sensation, fish also have another form of "distant touch" through the mechanosensory lateral line (Dijkgraaf, 1963). The mechanosensory lateral line is a hair cell-based system in aquatic vertebrates that senses hydrodynamic information, such as that created by conspecifics (Butler and Maruska, 2015; Butler and Maruska, 2016a; Butler and Maruska, 2016b; Groneberg et al., 2020; Montgomery et al., 2013). In zebrafish, chemical ablation of the mechanosensory lateral line prevents the rescue of *pth2* expression by a social environment following isolation (Anneser et al., 2020). Therefore, social "touch" (direct contact in rodents and hydrodynamic communication in zebrafish) seems to be a primary sensory activator of *pth2* expression.

Despite this knowledge, there remain several unanswered questions regarding the social regulation of *pth2* expression. First, how do zebrafish interpret social context when they are born without lateral line function? Secondly, do mechanosensory hair cells in the inner ear contribute

74 to the ability of zebrafish larvae to respond to social context? Thirdly, is *pth2* expression regulated
75 solely via mechanosensation, or can fish use additional sensory inputs to sense the presence of
76 conspecifics? Here, we report that the congenital loss of mechanosensory hair cell function leads
77 to chronically depressed levels of *pth2* expression in socially-housed larval zebrafish.
78 Interestingly, social isolation of hair cell mutants further decreases *pth2* levels, suggesting that
79 larval fish use additional sensory information to sense conspecifics and modulate *pth2* expression.
80 Lastly, we utilize fluorescent reporters driven by the *pth2* regulatory region to evaluate the
81 morphology of *pth2*-expressing cells and visualize *pth2* dynamics *in vivo*. Overall, this study offers
82 additional insight into the sensory basis for social interactions in zebrafish and introduces novel
83 tools to track *pth2* expression in living fish.
84
85 **RESULTS**
86 **Decreased *pth2* expression in lateral line-deficient larval zebrafish.**
87 *pth2* expression in the thalamus decreases when fish are raised in isolation but increases
88 following a brief period of social interaction with conspecifics. However, when the
89 mechanosensory lateral line is ablated in isolated fish prior to social exposure, *pth2* expression
90 levels remain low (Anneser et al., 2020). This implicates the lateral line sensory system in
91 recognizing conspecifics to stimulate *pth2* expression. To further evaluate the role of the lateral
92 line in social recognition, we raised lateral line-deficient mutants (*lhfpl5b*$^{-/-}$) and their siblings in
93 separate social groups and detected *pth2* expression by mRNA *in situ* hybridization (ISH) at 4 days
94 post-fertilization (dpf). Socially-raised lateral line mutants exhibit a decrease in *pth2* expression
95 (M = 9.7, SD = 4.3) compared to wild type (WT) siblings (M = 29.9, SD = 1.7) (Fig. 1B, C), in
96 terms of a qualitative decrease in the intensity of staining as well as a significant decrease in the
97 number of detectable *pth2*-positive cells (Fig. 1D; One-tailed Welch's t-test, t = 18.25, P =
98 1.04×10^{-15}, Cohen d = 6.18). We also ablated lateral line hair cells in socially-raised WT larvae
99 using repeated neomycin treatments between 3 – 4 dpf (Venuto and Erickson, 2021) (Fig. 1E, Fig.
100 S1). Even though these larvae had social experience prior to losing lateral line input, neomycin-
101 treated larvae exhibit a significant decrease in the number of *pth2*-positive cells compared to
102 untreated controls (Fig. 1F; One-tailed Welch's t-test, t = 6.44, P = 1.21×10^{-7}, Cohen d = 3.22).
103 These results confirm that a loss of lateral line function, whether genetically or chemically-
104 induced, impairs the ability of *pth2* cells to respond to social context.

105 **Lack of evidence for modulation of *pth2* expression by mechanosensory inputs from inner**
106 **ear hair cells.**
107 Low levels of *pth2* expression remain in socially-raised lateral line mutants (Fig. 1B, C).
108 To determine if mechanosensory input from the inner ear was responsible for this remaining *pth2*
109 expression, we used three different types of mutations that disable hair cells of both the lateral line
110 and inner ear to compare to the lateral line mutant (*lhfpl5b*$^{-/-}$) and wild type zebrafish. Two of these
111 mutations (*pcdh15a*$^{-/-}$ and *tomt*$^{-/-}$) render the mechano-electrical transduction channel
112 nonfunctional in all hair cells, similar to how the *lhfpl5b* mutation specifically disables lateral line
113 hair cells (Erickson et al., 2017; Erickson et al., 2020; Maeda et al., 2017). The third mutant
114 disables the voltage-gated calcium channel in all hair cells (*cacna1da*$^{-/-}$), thereby blocking
115 stimulus-dependent glutamate release (Sheets et al., 2012; Sidi et al., 2004). Again, we measured
116 *pth2* expression via mRNA ISH (Fig. 2B-F) as well as quantitative PCR (qPCR) at 4 dpf (Fig. 2G).
117 Consistent with our ISH results from Fig. 1, each class of hair cell mutant exhibits a significant
118 decrease in *pth2* expression compared to their wild type siblings when raised socially (Fig. S2;
119 One-tailed Welch's t-test; *lhfpl5b*: t = 5.929, P = 0.011, Cohen d = 4.84; *tomt*: t = 3.857, P =
120 0.0305, Cohen d = 3.15; *cacna1da*: t = 5.154, P = 0.0044, Cohen d = 4.21). However, the pan-hair
121 cell mutants (*tomt*, *cacna1da*) did not differ in *pth2* expression levels compared to the lateral line-
122 only mutant (*lhfpl5b*) (Fig. 2G; One-way ANOVA; Mutant: F = 2.425, P = 0.169; Wild Type: F
123 = 0.791, P = 0.496). Because pan-hair cell mutants and lateral line-only mutants are
124 indistinguishable in terms of *pth2* expression levels, we conclude that inner ear mechanosensory
125 hair cells do not significantly contribute to the regulation of *pth2* expression in this context.
126
127 **Social isolation further reduces *pth2* expression in sensory hair cell mutants.**
128 Chemosensory and visual perception of conspecifics does not significantly rescue *pth2*
129 expression in larval zebrafish raised in isolation (Anneser et al., 2020). However, since disabling
130 both the lateral line and the inner ear does not completely eliminate *pth2* expression, other non-
131 hair cell-based sensory systems may contribute to the modulation of *pth2* by social context. To test
132 this, we compared *pth2* expression in social and isolated *lhfpl5b* and *tomt* mutants by both mRNA
133 ISH (Fig. 3A-C) and qPCR at 4 dpf (Fig. 3D). If *pth2* responds to conspecific signals solely via
134 the lateral line, we expect to see equivalently low expression in mutants raised in social and
135 isolated environments. However, we find this not to be the case. Social environment has a

136 significant effect on *pth2* expression, as isolated *lhfpl5b* and *tomt* mutants express less *pth2* than
137 social mutant siblings (Two-way ANOVA; *lhfpl5b:* $F = 16.42$, $P = 0.007$; *tomt*: $F = 65.53$, $P =$
138 0.00019). Genotype does not have a significant effect on *pth2* levels when larvae are raised in
139 isolation, as isolated mutants and isolated wild types are statistically indistinguishable (Two-way
140 ANOVA; *lhfpl5b:* $F = 2.65$, $P = 0.154$; *tomt*: $F = 0.873$, $P = 0.386$). Because social isolation further
141 reduces *pth2* expression in lateral line mutants, we conclude that *pth2* likely responds to
142 multisensory input during social experience.
143
144 **Morphology of *pth2*-expressing cells using fluorescent reporters.**
145 Fluorescent reporters provide information about the morphology and function of cells,
146 along with the ability to quantify gene expression in living organisms (Choe et al., 2021; Soboleski
147 et al., 2005). Therefore, we created stable lines of transgenic zebrafish expressing GFP or RFP
148 under control of the presumptive *pth2* promoter (Fig. 4 and Movie S1). Imaging of socially-reared,
149 transgenic larvae reveals the two bilateral cell clusters with complex projection patterns (Fig. 4A,
150 B). The anterior ipsilateral projections partially converge into a dense neuropil in the forebrain,
151 while other fibers project ventrally and posteriorly toward the midbrain. We also find ventral
152 projections that cross the midline between the two cell clusters. The projection patterns of the
153 neurites and number of cells are similar for both the GFP and RFP transgenes (Fig. S3; GFP: M =
154 38.5, SD = 2.8; RFP: M = 37.1, SD = 2.6; Two-tailed Welch's t-test; $t = 1.422$, $P = 0.166$, Cohen
155 $d = 0.519$). Combining counts from both clusters, there is an overall average of 40.3 cells per
156 individual (SD = 2.27). The cells within each cluster exhibit a range in fluorescent intensity, and
157 over half of the cells fall within the two lowest intensity bins (Fig 4C, D; M = 27.9, SD = 3.42).
158
159 **The *pth2* transgenes respond to social context and lateral line input.**
160 Next, we tested if the *pth2* transgenes respond to social context and lateral line input like
161 endogenous *pth2* (Fig. 5). Consistent with our mRNA ISH and qPCR results, isolated
162 *Tg(pth2:TagRFP)unb3* larvae exhibit a significant decrease in the average number of TagRFP-
163 positive, *pth2* cells (false-colored green) (M=28.3, SD = 2.8) relative to socially-reared siblings
164 (M = 37.3, SD = 2.6) at 4 dpf (Fig. 5A-C: One-tailed Welch's t-test; $t = 8.949$, $P = 5.42\text{x}10^{-10}$,
165 Cohen $d = 3.27$). Similarly, social *Tg(pth2:EGFP)unb2*; *lhfpl5b*$^{vo35/vo35}$ larvae have fewer
166 fluorescent cells on average (M = 34.2, SD = 2.8) than their social, WT siblings (M = 43.2, SD =

167 3.9) (Fig. 5D-F; One-tailed Welch's t-test; t = 6.421, P = 1.55x10^{-6}, Cohen d = 2.62). To gauge
168 whether isolation specifically diminishes expression from the *pth2*-driven transgenes, we
169 compared the effect of social isolation on transgene expression in *Tg(pth2:TagRFP)unb3;*
170 *Tg(slc6a3:EGFP)ot80* double transgenic larvae. The *slc6a3:EGFP* transgene expresses GFP
171 under control of the dopamine transporter (DAT) promoter in several discrete regions of the
172 zebrafish brain (Xi et al., 2011), including a population of dopaminergic cells in the pretectum
173 lying just dorsal to the *pth2*-expressing cells. If social context specifically modulates expression
174 from the *pth2:TagRFP* transgene, we expect that isolation will have no effect on the number of
175 neighboring dopaminergic cells. Indeed, the number of GFP-positive, dopaminergic cells (false-
176 colored magenta) in the pretectum do not change in response to social context (Fig. 5A-C; WT
177 Soc: M = 44.0, SD = 4.3; WT Iso: M = 45.1, SD = 4.7; One-tailed Welch's t-test, t = -0.654, P =
178 0.741, Cohen d = 0.239). These experiments demonstrate that the *pth2* transgenes specifically
179 respond to both social context and lateral line input. However, we note that the effects of isolation
180 and lateral line-deficiency on the *pth2* transgenes are not as pronounced as their effects on
181 endogenous *pth2* mRNA expression (Figs. 1 and 2). To test whether this discrepancy is due to the
182 high stability of green and red fluorescent proteins (Sacchetti et al., 2001; Verkhusha et al., 2003),
183 we compared the number of GFP-positive cells at 4 dpf when we begin isolation at 1 dpf vs. 2 dpf
184 (Fig. S4). We find that increasing the duration of isolation does not significantly change the
185 number of GFP-positive cells (1 dpf Iso: 29.8, SD = 2.6; 2 dpf Iso: M = 29.3, SD = 3.4; Two-tailed
186 Welch's t-test; t = -0.371, P = 0.716, Cohen d = 0.166). This indicates that the discrepancy between
187 transgenic and endogenous *pth2* expression is not due to insufficient isolation time.
188
189 **DISCUSSION**
190 Previous work revealed that larval zebrafish use lateral line information to sense the
191 presence of conspecifics, leading to upregulation of the social hormone Pth2. Here, we show that
192 *pth2* levels are chronically depressed in socially-raised larvae born without lateral line function.
193 However, social isolation further reduces *pth2* levels in lateral line mutants, suggesting that other
194 socially-derived sensory information can modulate *pth2* expression.
195
196 **The mechanosensory lateral line mediates *pth2* expression.**

197 Anneser, et al. (2020) implicated hydrodynamic stimuli from conspecifics as a key social
198 cue that upregulates production of the neuropeptide Pth2. Isolated larvae with chemically ablated
199 lateral lines fail to upregulate *pth2* when returned to a social environment. In the present study, we
200 use mutant zebrafish with a congenital loss of lateral line function to confirm that hydrodynamic
201 information modulates *pth2* expression. Furthermore, we find that repeated chemical ablation of
202 the lateral line also impairs the ability of social larvae to express *pth2*, even when exposed to
203 conspecifics prior to loss of lateral line function. Our approach complements that of Anneser et al.
204 by providing genetic evidence that *pth2* is modulated by lateral line sensory information (Fig. 1).
205 We conclude that, in terms of Pth2 production, zebrafish born without a lateral line experience a
206 form of isolation even when raised in a social context.
207
208 **Auditory and vestibular stimuli do not modulate *pth2* expression in larval zebrafish.**
209 Inner ear hair cells are functionally and structurally similar to lateral line hair cells, and
210 fish use auditory and vestibular sensory information in a variety of behaviors (Bagnall and
211 Schoppik, 2018; Kohashi et al., 2012; Nicolson et al., 1998; Privat et al., 2019). Given that some
212 *pth2* expression remains in lateral line mutants, we examined whether sensory information from
213 the inner ear contributes to social modulation of *pth2.* Using zebrafish with mutations that disable
214 both inner ear and the lateral line hair cells, we find that there is no additional loss of *pth2*
215 expression compared to the lateral line-only mutant (Fig. 2). In addition, we asked if different types
216 of mutations to hair cells impact *pth2* expression. Three of the mutant lines used in this study,
217 *lhfpl5b, tomt* and *pcdh15a,* render the mechanotransduction (MET) channel non-functional
218 (Erickson et al., 2017; Erickson et al., 2020; Maeda et al., 2017), and one mutant line, *cacna1da /*
219 *cav1.3a,* affects the voltage-gated calcium channel (Sheets et al., 2012; Sidi et al., 2004). All
220 mutant alleles are recognized as nulls since mutant hair cells show little to no residual
221 mechanosensory activity, as demonstrated by the lack of evoked spikes in the posterior lateral line
222 ganglion, the absence of microphonic potentials and mechanotransduction currents, or the absence
223 of MET channel-dependent FM dye labeling of hair cells (Nicolson et al., 1998; Erickson et al.,
224 2017; Erickson et al., 2020; Sidi et al., 2004). While the MET channel and calcium channel are
225 both necessary components for proper hair cell signal transduction, there are key differences
226 between the types of mutations. For mutants affecting the MET channel, potassium and calcium
227 ions are unable to enter the cell in response to stimuli, but the potential for spontaneous calcium

228 influx and neurotransmitter release remains (Trapani and Nicolson, 2011). Whereas for the
229 calcium channel mutation, ions enter through the MET channel but there is no evoked or
230 spontaneous neurotransmitter release. Regardless, all mutations that disrupt hair cell function
231 result in the same decrease of *pth2* expression in socially raised fish compared to their wild type
232 siblings (Fig. 2). Therefore, we conclude that regulation of *pth2* by social context is primarily via
233 the mechanosensory lateral line in larval zebrafish and that auditory and vestibular information
234 likely does not contribute.
235
236 **Additional socially-derived sensory cues modulate *pth2* expression.**
237 Anneser et al. (2020) demonstrated that neither chemical nor visual cues from conspecifics
238 significantly restored *pth2* expression in isolated larvae. In our study, we found that isolation
239 further reduced *pth2* expression in lateral line mutants to the same level as isolated wild types (Fig.
240 3). This indicates that additional sensory modalities contribute to the regulation of *pth2* expression.
241 Recent studies have identified thalamic neurons in the zebrafish that respond to biological motion
242 and shown that these neurons are molecularly defined by the partially overlapping expression of
243 *pth2* and *cortistatin* (*cort* / *sst7*) (Kappel et al., 2022; Sherman et al., 2021). It will be informative
244 to test whether photo- or chemosensory systems can modulate *pth2* expression under sensitized
245 circumstances in which hydrosensory information is compromised. Additionally, it is possible that
246 tactile stimuli are contributing to *pth2* regulation in zebrafish, consistent with the effects of social
247 touch in rodents. Future work is necessary to test this theory.
248
249 **Visualizing *pth2* expression *in vivo.***
250 We used *pth2* promoter-driven fluorescent transgenes to visualize *pth2*-expressing cells
251 and their projections. Consistent with the Anneser et al. (2020) whole-mount immunostains, we
252 see Pth2-positive cells located in bilateral clusters in the thalamus that feature lateral neurites,
253 anterior ipsilateral projections terminating as a loosely organized neuropil in the telencephalon, as
254 well as posterior ipsilateral projections. The transgene reveals additional fibers that project
255 ventrally from the cell bodies and cross the midline, potentially contacting the contralateral *pth2*-
256 expressing cluster (Fig. 4 and Movie S1). Investigating the morphology of these cells will help us
257 understand the cellular targets of Pth2 signaling and how activity of the two clusters is coordinated.
258 We note an excess of putative *pth2*-expressing cells in the transgenics compared to our ISH

259 experiments and the immunostain counts of Anneser et al. (2020). This discrepancy could be due,
260 in part, to the increased sensitivity of using confocal microscopy to detect *pth2*-expressing cells in
261 a live transgenic animal as opposed to imaging fixed tissue stained for mRNA or protein.
262 Consistent with this idea, we find that the majority of GFP-positive cells in socially-reared
263 *Tg(pth2:EGFP)* larvae exhibit low fluorescence intensity (Fig. 4C, D). If these dim transgenic cells
264 represent neurons that express *pth2* at a level below the detection limit of mRNA ISH or
265 immunostain, this may account for the excess cell counts in our transgenics.

266 We also tested the *pth2:EGFP* and *pth2:TagRFP* transgenic lines as a proxy for *pth2*
267 expression *in vivo* and found that both lateral line mutants and isolated wild type larvae exhibit
268 fewer fluorescent cells than socially raised siblings (Fig. 5). In contrast, the number of
269 dopaminergic cells located dorsally to the *pth2* clusters exhibit no change to social context.
270 Dopamine has been implicated in social interactions (Haehnel-Taguchi et al., 2018; Saif et al.,
271 2013; Shams et al., 2018), so we used the nearby clusters of GFP-labeled dopaminergic cells in
272 the *slc6a3:EGFP* transgenic line to test the specificity of the response of the *pth2* transgene to
273 social context. Our results indicate that the social modulation of *pth2* is specific and distinct from
274 the dopaminergic system in this brain region of larval zebrafish.

275 While our results with the *pth2* transgenes agree with our *in situ* hybridization and qPCR
276 results (Figs. 1-3), we note that the effects of isolation and lateral line deficiency on transgene
277 expression are not as prominent as when assaying for endogenous *pth2* mRNA and protein. As
278 mentioned above, the enhanced detectability of genetically-encoded reporters in live larvae may
279 account for some of the residual fluorescence that remains following social isolation of
280 transgenics. It could also be that the post-transcriptional and / or post-translational stability of the
281 fluorescent transgenes differ from endogenous *pth2* mRNA and protein stability. We tested
282 whether the long half-life of GFP accounts for the persistence of GFP-positive cells in isolated
283 *Tg(pth2:EGFP)* larvae but found that extending the duration of isolation from 48 to 72 hours did
284 not significantly affect the number of fluorescent cells (Fig. S4). Lastly, it is possible that
285 additional regulatory elements in the *pth2* promoter or 3' UTR, along with the use of a destabilized
286 fluorescent protein, are required to mimic the endogenous regulation of *pth2*. Future work will
287 strive to distinguish between these possibilities and to optimize the transgene for more accurate
288 reporting of *pth2* dynamics in vivo.

289 Overall, our results confirm that *pth2* expression is modulated by the mechanosensory
290 lateral line (Fig. 1). We also show that the lateral line is the only hair-cell based sensory organ
291 regulating *pth2* expression (Fig. 2). However, due to expression levels being slightly higher in
292 social lateral line mutants compared to the same mutants or wild type larvae raised in isolation, we
293 conclude that there must be unidentified sensory system(s) that contribute to the modulation of
294 *pth2* (Fig. 3). Finally, we created transgenic lines to visualize the morphology of *pth2*+ cells *in*
295 *vivo* (Fig. 4), and report that the transgenes respond to social context (Fig. 5). These transgenic
296 lines can be used in future studies to elucidate the role of *pth2* in zebrafish. Taken together, this
297 work suggests that zebrafish without a functioning lateral line experience a form of isolation, even
298 in a social context.
299

300 **MATERIALS AND METHODS**

301 **Ethics statement**

302 Animal research complied with guidelines stipulated by the Institutional Animal Care and
303 Use Committees at East Carolina University (Greenville, NC, United States) and at University of
304 New Brunswick (Fredericton, New Brunswick, Canada). Zebrafish (*Danio rerio*) were maintained
305 and bred using standard procedures (Westerfield, 2000). All experiments used larvae at 1–5 days
306 post-fertilization (dpf), which are of indeterminate sex at this stage.
307

308 **Mutant and transgenic fish lines**

309 The following previously described zebrafish mutant and transgenic lines were used in this
310 study: *lhfpl5b*^{vo35}, *pcdh15a*^{th263b}, *tomt*^{tk256c}, *cacna1da*^{tc323d}, and *Tg(slc6a3:EGFP)ot80* (Erickson et
311 al., 2017; Erickson et al., 2020; Maeda et al., 2017; Sidi et al., 2004; Xi et al., 2011). To make the
312 *Tg(pth2:EGFP)unb2* and *Tg*(*pth2:TagRFP)unb3* transgenic lines, 2067 base pairs immediately
313 upstream of the *pth2* coding region (including the 5' UTR and first intron) were PCR amplified
314 with primers containing attB4-B1 recombination sites (*pth2*-specific sequence underlined: Fwd:
315 GGGGACAACTTTGTATAGAAAAGTTGGTAAAGGACACTCTTTGAGATCCT, Rvs:
316 GGGGACTGCTTTTTTGTACAAACTTGCCTGCAGATGAATAAGTTGAATAATACA. The
317 PCR product was cloned into the Gateway pDONR-P4-P1R entry vector by a standard BP clonase
318 reaction and a Multisite LR reaction was performed to create *pth2:EGFP-pA, cryaa:EGFP* and
319 *pth2:tagRFP-pA, cryaa:mCherry* plasmids. pDestTol2pACryGFP and pDESTtol2pACrymCherry

320 plasmids were gifts from Joachim Berger & Peter Currie (Addgene plasmids # 64022, 64023). The
321 expression constructs were co-injected with *tol2* transposase mRNA into 1-cell zebrafish embryos
322 (Kwan et al., 2007). F0 founders were outcrossed to produce stable F1 transgenics. At a minimum,
323 progeny from F2 transgenics were used in this study.
324
325 **Mutant and social isolation experiments for *in situ* hybridization, qPCR, and transgenic lines**
326 Zebrafish larvae were sorted for *lhfpl5b*^{vo35}, *pcdh15a*^{th263b}, *tomt*^{tk256c} homozygotes at 2 dpf
327 with FM1-43 dye labelling for social isolation experiments. *cacna1da*^{tc323d} homozygotes were
328 identified behaviorally by the "circler" phenotype at 4 dpf (Nicolson, et al., 1998), as they cannot
329 be identified by differential FM1-43 dye labeling and were not used in isolation experiments.
330 *Tg*(*pth2:EGFP)* and *Tg*(*pth2:TagRFP)* transgenics were identified by their GFP or mCherry lens
331 markers, respectively. *Tg(slc6a3:EGFP)* transgenics were identified by GFP expression in the
332 brain. Identified larvae were divided into social groups of thirty, while another thirty larvae were
333 placed in isolation, except for *cacna1da*^{tc323d} larvae which were only raised socially. Both social
334 and isolated larvae were housed in 6-well tissue culture plates containing 5 ml of E3 embryo media.
335 For the social condition, all 30 larvae were placed in one well with 5 ml of embryo media. For the
336 isolated condition, one larva was placed per well with 5 ml of embryo media. Strips of paper were
337 placed between each well to prevent visual access between wells. Larvae intended for mRNA *in*
338 *situ* hybridization (ISH) were grown in E3 with 200 µM N-Phenylthiourea (PTU) (Alfa Aesar) to
339 prevent pigment formation. Each group was incubated at 28.5ºC with a 14L:10D photoperiod from
340 2 to 4 dpf. At 4 dpf, larvae were either fixed for *in situ* hybridization, processed for qPCR, or
341 imaged to visualize the transgene.
342
343 **Repeated neomycin treatments**
344 The repeated neomycin treatments were performed essentially as previously described
345 (Venuto & Erickson, 2021). At 24 hpf, WT embryos were divided into groups of 30 and grown
346 continuously in the dark at 28.5ºC in media supplemented with 200 µM PTU to prevent pigment
347 formation. Larvae were manually dechorionated at 2 dpf. Starting at 9:00 AM, 3 dpf larvae were
348 exposed to either 0 or 50 µM neomycin sulfate hydrate (Alfa Aesar) for 30 minutes at 28.5ºC every
349 12 hours for a total of three treatments. At noon on 4 dpf, treated and untreated groups of larvae
350 were anesthetized with 0.016% MS-222 and fixed in 4% PFA for mRNA ISH. The experiments

351 were repeated three times, each with two technical replicates for the control and treatment groups.
352 Three hours after treatment 1, ablation of lateral line hair cells was assessed by incubating 3 dpf
353 larvae in 130 µM DASPEI (2-[4-(dimethylamino)styryl]-1-ethylpyridinium iodide) for 10
354 minutes. Following three washes with E3, larvae were anesthetized with 0.016% MS-222,
355 positioned laterally on a depression slide in 1.2% low melting point agarose, and imaged with a
356 Basler Ace 5.1 MP color camera on a Zeiss SV-11 microscope using an X-Cite 120Q illuminator
357 and wideband GFP filter.
358
359 **mRNA in situ hybridization**
360 The *pth2* in situ probe sequence was amplified using the Invitrogen SuperScript IV One-
361 Step RT-PCR kit (ThermoFisher) using the following forward and reverse primers: F:
362 CATTGCATGGACGATTTACG; R: TGCCATGTCATTCAAAATCC. The RT-PCR product
363 was purified by gel extraction and propagated in the pCR4-TOPO vector. The pCR4-*pth2* plasmid
364 was linearized with NotI and the antisense DIG-labeled ISH probe was synthesized using the T3
365 RNA polymerase promoter. Probe synthesis and in situ hybridization were performed essentially
366 as described (Erickson et al., 2010). Larvae were imaged at 20X magnification using either an
367 Olympus BH-2 microscope outfitted with a Jenoptik Gryphax Arktur camera or a Nikon Eclipse
368 50i microscope with a Basler Ace 5.1 MP color camera. ISH cell counts were conducted in a non-
369 blinded manner by manually focusing through a mounted larvae prior to capturing a static image.
370
371 **RNA isolation and real time quantitative PCR (qPCR)**
372 For RNA isolation, ten larval heads were used per biological replicate. Samples were
373 collected on ice, placed in 1.7 mL RNase-free microcentrifuge tubes containing 200 µl RNAzol
374 (Molecular Research Center, Inc., OH. Catalog: RN 190) and homogenized immediately. This was
375 repeated for a total of three biological replicates. Total RNA was extracted from homogenized
376 solutions according to the manufacturer's protocol. For each sample, cDNAs was synthesized
377 using 1 µg total RNA and a high-capacity cDNA Reverse Transcription kit (Thermo Fisher
378 Scientific, Waltham, Massachusetts, USA, Catalog# 4368814) following the manufacturer's
379 instructions.
380 The levels of *pth2* transcripts were determined by quantitative real-time PCR (qPCR) using
381 SYBR green dye (Invitrogen) and a CFX Connect real-time thermal cycler (Bio-Rad Laboratories,

382 Hercules, California, USA). The qPCR reaction was conducted with initial denaturation at 95 °C
383 for 2 min, followed by 30 cycles of 30 s denaturation at 95 °C, 30 s annealing at 57 °C, and 30 s
384 extension at 72 °C using the specific primers (Forward: CCACGCAACACACAGTCAAG,
385 Reverse: GCAAGTTACTTTGCAGAGGTC) and GoTaq G2 DNA polymerase (Promega,
386 Madison, Wisconsin, USA). Each PCR mixture (15 µl) consisted of 7.795 µl DNase free water,
387 3 µl 5X GoTaq buffer, 1.5 µl 25 mM MgCl2, 0.3 µl 10 mM dNTP mix, 0.15 ml 10µM forward or
388 reverse primer, 2 µl cDNA, 0.03 µl 100X SYBR green dye (final concentration 0.2X), and 0.075
389 µl Taq. Two technical replicates per biological replicate were averaged together for analysis.
390 Absolute values (copies/µg total RNA) were determined using Ct values of samples and a standard
391 curve generated from serial known concentrations of plasmid containing the target region of *pth2*.
392 Relative expression was found by calculating the fold change compared to the mean value of the
393 isolated, wild type condition. The efficiency of the PCR and authentic PCR products was further
394 confirmed by analyses of melting curve and gel electrophoresis.
395
396 **Transgenic imaging and quantification**
397 Live zebrafish larvae were anesthetized with 0.016% MS-222 in E3 and mounted dorsally
398 on a depression slide in 1.2% low melting point agarose in E3. EGFP was imaged using a Zeiss
399 LSM800 laser-scanning confocal with a 40x water objective and Zeiss Zen software. To quantify
400 results, cell counts were performed using Fiji/ImageJ image processing software (Schindelin et al.,
401 2012). Cells were counted in a non-blinded manner by manually going through the z-stacks. The
402 cell count process was repeated twice at a minimum to ensure accuracy. Images shown are
403 maximum intensity projections of z-stacks. For the fluorescent intensity experiment, the intensity
404 of each cell was collected from a sum slices z-projection in Fiji/ImageJ and the integrated density
405 values were used for analysis. Depth encoded 2D and 3D projections were created in Fiji/ImageJ
406 using the *Z-stack Depth Color Code 0.0.2* plugin. Figures were assembled in Adobe Photoshop
407 and equally adjusted for brightness and contrast among corresponding treatment groups.
408
409 **Statistical tests**
410 All graphs and statistical tests were done using R (R Core Team, 2021). For *in* situ
411 hybridization cell counts, a one-tailed Welch's t-test was used (two biological replicates, n = 7-9
412 larvae per condition per replicate). For the qPCR experiment comparing the various hair cell

mutants raised socially (Fig. 2), a one-way ANOVA was conducted (three biological replicates, n = 10 per condition per replicate). For the same experiment comparing wild type versus mutant larvae raised socially, a one-tailed Welch's t-test was used to compare within mutant lines. For the qPCR experiment comparing genotypes and social status (Fig. 3), a two-way ANOVA was conducted (three biological replicates, n = 10 per condition per replicate). For the transgenic cell counts, a one-tailed Welch's t-test was used (three biological replicates, n = 5 per condition per replicate), except for the 1 dpf versus 2 dpf and GFP versus RFP cell counts where we used two-tailed Welch's t-test to test significance. A p-value of less than 0.05 was considered significant. The more stringent one-tailed t-tests were used due to only having an expectation for a decrease in *pth2* expression following isolation or loss of lateral line sensory information. Sample sizes were determined by the number of fish used in the experiment and no samples were excluded from the analysis. Pre-determined criteria to exclude samples included if the fish was not touch-responsive or displayed obvious developmental abnormalities.

ACKNOWLEDGMENTS

The authors would like to thank Dr. Yong Zhu (ECU) for reagents and assistance with qPCR experiments, Dr. Les Cwynar (UNB) for use of his microscope, and Dr. Bryan Crawford (UNB) for reagents and helpful comments on the manuscript. We also thank members of the Erickson and Issa labs for their assistance with zebrafish husbandry.

COMPETING INTERESTS

The authors declare no competing interests.

FUNDING

This work was funded by East Carolina University's Division of Research, Economic Development and Engagement (REDE), the New Brunswick Innovation Foundation (NBIF), and the Natural Science and Engineering Research Council (NSERC) of Canada Discovery Grant RGPIN-2021-03166 to T.E.

DATA AVAILABILITY

The datasets generated for this study are available on request to the corresponding author.

REFERENCES

Adkins-Regan, E. (2009). Neuroendocrinology of social behavior. *ILAR J* **50**, 5–14.

Amaral, D. G. (2002). The primate amygdala and the neurobiology of social behavior: implications for understanding social anxiety. *Biol Psychiatry* **51**, 11–17.

Anneser, L., Alcantara, I. C., Gemmer, A., Mirkes, K., Ryu, S. and Schuman, E. M. (2020). The neuropeptide Pth2 dynamically senses others via mechanosensation. *Nature 2020 588:7839* **588**, 653–657.

Anneser, L., Gemmer, A., Eilers, T., Alcantara, I. C., Loos, A.-Y., Ryu, S. and Schuman, E. M. (2022). The neuropeptide Pth2 modulates social behavior and anxiety in zebrafish. *iScience* **25**, 103868.

Bagnall, M. W. and Schoppik, D. (2018). Development of vestibular behaviors in zebrafish. *Curr Opin Neurobiol* **53**, 83.

Bhattacharya, P., Yan, Y. L., Postlethwait, J. and Rubin, D. A. (2011). Evolution of the vertebrate pth2 (TIP39) gene family and the regulation of PTH type 2 receptor (pth2r) and its endogenous ligand pth2 by hedgehog signaling in zebrafish development. *Journal of Endocrinology* **211**, 187–200.

Brothers, L. (1990). The neural basis of primate social communication. *Motivation and Emotion 1990 14:2* **14**, 81–91.

Burgdorf, J. and Panksepp, J. (2006). The neurobiology of positive emotions. *Neurosci Biobehav Rev* **30**, 173–187.

Butler, J. M. and Maruska, K. P. (2015). The mechanosensory lateral line is used to assess opponents and mediate aggressive behaviors during territorial interactions in an African cichlid fish. *J Exp Biol* **218**, 3284–94.

Butler, J. M. and Maruska, K. P. (2016a). The Mechanosensory Lateral Line System Mediates Activation of Socially-Relevant Brain Regions during Territorial Interactions. *Front Behav Neurosci* **10**, 93.

Butler, J. M. and Maruska, K. P. (2016b). Mechanosensory signaling as a potential mode of communication during social interactions in fishes. *J Exp Biol* **219**, 2781–2789.

Chen, P. and Hong, W. (2018). Neural Circuit Mechanisms of Social Behavior. *Neuron* **98**, 16–30.

Choe, C. P., Choi, S.-Y., Kee, Y., Kim, M. J., Kim, S.-H., Lee, Y., Park, H.-C. and Ro, H. (2021). Transgenic fluorescent zebrafish lines that have revolutionized biomedical research. *Laboratory Animal Research 2021 37:1* **37**, 1–29.

Coutellier, L. and Usdin, T. B. (2011). Enhanced long-term fear memory and increased anxiety and depression-like behavior after exposure to an aversive event in mice lacking TIP39 signaling. *Behavioural Brain Research* **222**, 265–269.

Cservenák, M., Szabó, É. R., Bodnár, I., Lékó, A., Palkovits, M., Nagy, G. M., Usdin, T. B. and Dobolyi, A. (2013). Thalamic neuropeptide mediating the effects of nursing on lactation and maternal motivation. *Psychoneuroendocrinology* **38**, 3070–3084.

Dijkgraaf, S. (1963). The functioning and significance of the lateral-line organs. *Biological Reviews* **38**, 51–105.

Dimitrov, E. and Usdin, T. B. (2010). Tuberoinfundibular peptide of 39 residues modulates the mouse hypothalamic-pituitary-adrenal axis via paraventricular glutamatergic neurons. *J Comp Neurol* **518**, 4375–4394.

Dimitrov, E. L., Petrus, E. and Usdin, T. B. (2010). Tuberoinfundibular peptide of 39 residues (TIP39) signaling modulates acute and tonic nociception. *Exp Neurol* **226**, 68–83.

490 **Dimitrov, E. L., Kuo, J., Kohno, K. and Usdin, T. B.** (2013). Neuropathic and inflammatory
491 pain are modulated by tuberoinfundibular peptide of 39 residues. *Proceedings of the*
492 *National Academy of Sciences* **110**, 13156–13161.
493 **Dobolyi, A., Dimitrov, E., Palkovits, M. and Usdin, T. B.** (2012). The Neuroendocrine
494 Functions of the Parathyroid Hormone 2 Receptor. *Front Endocrinol (Lausanne)* **3**, 121.
495 **Erickson, T., French, C. R. and Waskiewicz, A. J.** (2010). Meis1 specifies positional
496 information in the retina and tectum to organize the zebrafish visual system. *Neural Dev* **5**,
497 22.
498 **Erickson, T., Morgan, C. P., Olt, J., Hardy, K., Busch-Nentwich, E., Maeda, R., Clemens,**
499 **R., Krey, J. F., Nechiporuk, A., Barr-Gillespie, P. G., et al.** (2017). Integration of
500 Tmc1/2 into the mechanotransduction complex in zebrafish hair cells is regulated by
501 Transmembrane O-methyltransferase (Tomt). *Elife* **6**,.
502 **Erickson, T., Pacentine, I. v., Venuto, A., Clemens, R. and Nicolson, T.** (2020). The lhfpl5
503 Ohnologs lhfpl5a and lhfpl5b Are Required for Mechanotransduction in Distinct
504 Populations of Sensory Hair Cells in Zebrafish. *Front Mol Neurosci* **12**, 320.
505 **Groneberg, A. H., Marques, J. C., Martins, A. L., Diez del Corral, R., de Polavieja, G. G.**
506 **and Orger, M. B.** (2020). Early-Life Social Experience Shapes Social Avoidance
507 Reactions in Larval Zebrafish. *Current Biology* **30**, 4009-4021.e4.
508 **Haehnel-Taguchi, M., Fernandes, A. M., Böhler, M., Schmitt, I., Tittel, L. and Driever, W.**
509 (2018). Projections of the diencephalospinal dopaminergic system to peripheral sense
510 organs in larval zebrafish (Danio rerio). *Front Neuroanat* **12**, 20.
511 **Kappel, J. M., Förster, D., Slangewal, K., Shainer, I., Svara, F., Donovan, J. C., Sherman,**
512 **S., Januszewski, M., Baier, H. and Larsch, J.** (2022). Visual recognition of social signals
513 by a tectothalamic neural circuit. *Nature 2022 608:7921* **608**, 146–152.
514 **Keller, D., Láng, T., Cservenák, M., Puska, G., Barna, J., Csillag, V., Farkas, I., Zelena, D.,**
515 **Dóra, F., Barteczko, L., et al.** (2022). A thalamo-preoptic pathway promoting social touch.
516 *bioRxiv* 2022.01.11.475648.
517 **Kohashi, T., Nakata, N. and Oda, Y.** (2012). Effective Sensory Modality Activating an Escape
518 Triggering Neuron Switches during Early Development in Zebrafish. *The Journal of*
519 *Neuroscience* **32**, 5810.
520 **Kolb, B. and Whishaw, I. Q.** (2003). Brain Plasticity and Behavior.
521 *http://dx.doi.org/10.1146/annurev.psych.49.1.43* **49**, 43–64.
522 **Kravitz, E. A. and Huber, R.** (2003). Aggression in invertebrates. *Curr Opin Neurobiol* **13**,
523 736–743.
524 **Kwan, K. M., Fujimoto, E., Grabher, C., Mangum, B. D., Hardy, M. E., Campbell, D. S.,**
525 **Parant, J. M., Yost, H. J., Kanki, J. P. and Chien, C.-B.** (2007). The Tol2kit: a multisite
526 gateway-based construction kit for Tol2 transposon transgenesis constructs. *Dev Dyn* **236**,
527 3088–99.
528 **LaBuda, C. J. and Usdin, T. B.** (2004). Tuberoinfundibular peptide of 39 residues decreases
529 pain-related affective behavior. *Neuroreport* **15**, 1779–1782.
530 **LaBuda, C. J., Dobolyi, A. and Usdin, T. B.** (2004). Tuberoinfundibular peptide of 39 residues
531 produces anxiolytic and antidepressant actions. *Neuroreport* **15**, 881–885.
532 **Maeda, R., Pacentine, I. v., Erickson, T. and Nicolson, T.** (2017). Functional Analysis of the
533 Transmembrane and Cytoplasmic Domains of Pcdh15a in Zebrafish Hair Cells. *The Journal*
534 *of Neuroscience* **37**, 3231–3245.

535 **Montgomery, J., Bleckmann, H. and Coombs, S.** (2013). Sensory Ecology and Neuroethology
536 of the Lateral Line. 121–150.
537 **Mueller, T.** (2012). What is the Thalamus in Zebrafish? *Front Neurosci* **6**, 64.
538 **Mumtaz, F., Khan, M. I., Zubair, M. and Dehpour, A. R.** (2018). Neurobiology and
539 consequences of social isolation stress in animal model—A comprehensive review.
540 *Biomedicine & Pharmacotherapy* **105**, 1205–1222.
541 **Neumann, I. D., Veenema, A. H. and Beiderbeck, D. I.** (2010). Aggression and anxiety: Social
542 context and neurobiological links. *Front Behav Neurosci* **4**, 12.
543 **Nicolson, T., Rüsch, A., Friedrich, R. W., Granato, M., Ruppersberg, J. P. and Nüsslein-**
544 **Volhard, C.** (1998). Genetic Analysis of Vertebrate Sensory Hair Cell Mechanosensation:
545 the Zebrafish Circler Mutants. *Neuron* **20**, 271–283.
546 **O'Connell, L. A. and Hofmann, H. A.** (2011). Genes, hormones, and circuits: An integrative
547 approach to study the evolution of social behavior. *Front Neuroendocrinol* **32**, 320–335.
548 **Oldfield, R. G. and Hofmann, H. A.** (2011). Neuropeptide regulation of social behavior in a
549 monogamous cichlid fish. *Physiol Behav* **102**, 296–303.
550 **Panksepp, J. and Burgdorf, J.** (2003). "Laughing" rats and the evolutionary antecedents of
551 human joy? *Physiol Behav* **79**, 533–547.
552 **Panksepp, J., Burgdorf, J., Beinfeld, M. C., Kroes, R. A. and Moskal, J. R.** (2007). Brain
553 Regional Neuropeptide Changes Resulting From Social Defeat. *Behavioral Neuroscience*
554 **121**, 1364–1371.
555 **Privat, M., Romano, S. A., Pietri, T., Jouary, A., Boulanger-Weill, J., Elbaz, N., Duchemin,**
556 **A., Soares, D. and Sumbre, G.** (2019). Sensorimotor Transformations in the Zebrafish
557 Auditory System. *Current Biology* **29**, 4010-4023.e4.
558 **R Core Team** (2021). R: A Language and Environment for Statistical Computing.
559 **Robinson, G. E., Fernald, R. D. and Clayton, D. F.** (2008). Genes and social behavior. *Science*
560 **322**, 896–900.
561 **Sacchetti, A., el Sewedy, T., Nasr, A. F. and Alberti, S.** (2001). Efficient GFP mutations
562 profoundly affect mRNA transcription and translation rates. *FEBS Lett* **492**, 151–155.
563 **Saif, M., Chatterjee, D., Buske, C. and Gerlai, R.** (2013). Sight of conspecific images induces
564 changes in neurochemistry in zebrafish. *Behavioural Brain Research* **243**, 294–299.
565 **Schindelin, J., Arganda-Carreras, I., Frise, E., Kaynig, V., Longair, M., Pietzsch, T.,**
566 **Preibisch, S., Rueden, C., Saalfeld, S., Schmid, B., et al.** (2012). Fiji: an open-source
567 platform for biological-image analysis. *Nature Methods 2012 9:7* **9**, 676–682.
568 **Schoofs, L., de Loof, A. and van Hiel, M. B.** (2017). Neuropeptides as Regulators of Behavior
569 in Insects. *http://dx.doi.org/10.1146/annurev-ento-031616-035500* **62**, 35–52.
570 **Seitz, N.** (2019). Characterization Of Pth Type-2 Receptor (pth2rb) And Its Endogenous Ligand
571 Pth2 In Zebrafish Development. *Theses and Dissertations*.
572 **Shams, S., Seguin, D., Facciol, A., Chatterjee, D. and Gerlai, R.** (2017). Effect of social
573 isolation on anxiety-related behaviors, cortisol, and monoamines in adult zebrafish.
574 *Behavioral Neuroscience* **131**, 492–504.
575 **Shams, S., Amlani, S., Buske, C., Chatterjee, D. and Gerlai, R.** (2018). Developmental social
576 isolation affects adult behavior, social interaction, and dopamine metabolite levels in
577 zebrafish. *Dev Psychobiol* **60**, 43–56.
578 **Sheets, L., Kindt, K. S. and Nicolson, T.** (2012). Presynaptic CaV1.3 Channels Regulate
579 Synaptic Ribbon Size and Are Required for Synaptic Maintenance in Sensory Hair Cells.
580 *The Journal of Neuroscience* **32**, 17273.

Sherman, S., Kawakami, K. and Baier, H. (2021). Retinal input influences pace of neurogenesis but not cell-type configuration of the visual forebrain. *bioRxiv* 2021.11.15.468630.

Sidi, S., Busch-Nentwich, E., Friedrich, R., Schoenberger, U. and Nicolson, T. (2004). gemini Encodes a Zebrafish L-Type Calcium Channel That Localizes at Sensory Hair Cell Ribbon Synapses. *The Journal of Neuroscience* **24**, 4213.

Soboleski, M. R., Oaks, J. and Halford, W. P. (2005). Green fluorescent protein is a quantitative reporter of gene expression in individual eukaryotic cells. *The FASEB journal : official publication of the Federation of American Societies for Experimental Biology* **19**, 440.

Trapani, J. G. and Nicolson, T. (2011). Mechanism of Spontaneous Activity in Afferent Neurons of the Zebrafish Lateral-Line Organ. *The Journal of Neuroscience* **31**, 1614.

Venuto, A. and Erickson, T. (2021). Evaluating the Death and Recovery of Lateral Line Hair Cells Following Repeated Neomycin Treatments. *Life* **11**, 1180.

Verkhusha, V. v., Kuznetsova, I. M., Stepanenko, O. v., Zaraisky, A. G., Shavlovsky, M. M., Turoverov, K. K. and Uversky, V. N. (2003). High stability of Discosoma DsRed as compared to Aequorea EGFP. *Biochemistry* **42**, 7879–7884.

Weiss, I. C., Pryce, C. R., Jongen-Rêlo, A. L., Nanz-Bahr, N. I. and Feldon, J. (2004). Effect of social isolation on stress-related behavioural and neuroendocrine state in the rat. *Behavioural Brain Research* **152**, 279–295.

Westerfield, M. (2000). *The zebrafish book. A guide for the laboratory use of zebrafish (Danio rerio).* 4th ed. Eugene OR: University of Oregon.

Xi, Y., Yu, M., Godoy, R., Hatch, G., Poitras, L. and Ekker, M. (2011). Transgenic zebrafish expressing green fluorescent protein in dopaminergic neurons of the ventral diencephalon. *Developmental Dynamics* **240**, 2539–2547.

608 **FIGURES AND LEGENDS:**

609

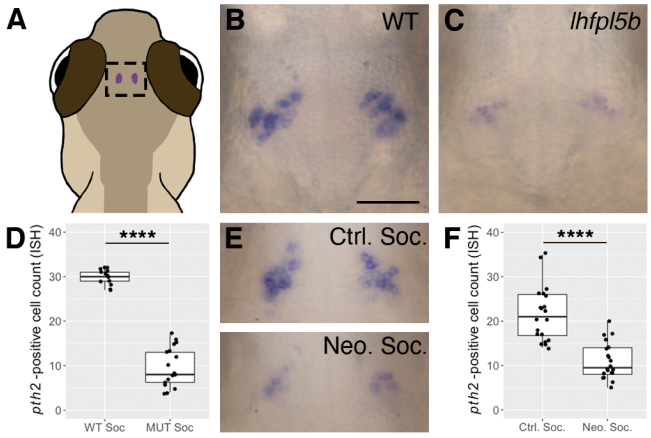

610

611 **Fig. 1: Decreased *pth2* expression in lateral line-deficient zebrafish larvae.** (A) Location of
612 *pth2*-expressing cells in the thalamic region of a larval zebrafish. (B-C) Representative images of
613 mRNA *in situ* hybridizations (ISH) showing *pth2*-positive cells in socially-reared wild type and
614 lateral line mutant (*lhfpl5b*^{vo35}) larvae at 4 dpf. (D) Boxplots of *pth2*-positive cell counts from ISH
615 images of *lhfpl5b* larvae at 4 dpf (WT = 14, MUT = 18 larvae from two replicates). (E)
616 Representative mRNA ISH images from socially-reared control (Neo. ctrl) and neomycin-treated
617 (Neo. trt.) larvae at 4 dpf showing reduced *pth2* expression following repeated chemical ablation
618 of the lateral line hair cells. (F) Boxplots of *pth2*-positive cell counts from control and neomycin-
619 treated larvae at 4 dpf (Control = 20, Treated = 20 larvae pooled from two replicates). Scale bar in
620 B is 50 µm and applies to all images. A one-tailed Welch's t-test was used to assess significance,
621 **** = $p < 0.0001$.

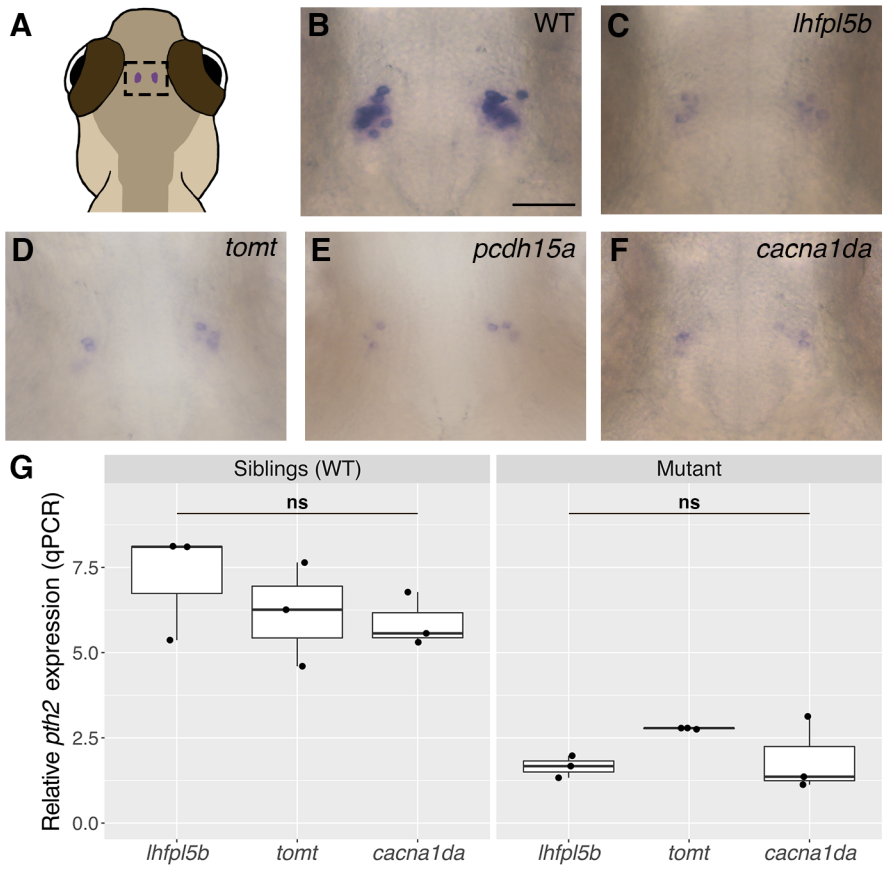

Fig. 2: Lack of evidence for modulation of *pth2* expression by mechanosensory inputs from inner ear hair cells. (A) Location of *pth2*-expressing cells in the thalamic region of a larval zebrafish. (B-F) Representative images of mRNA *in situ* hybridizations (ISH) showing *pth2*-positive cells in socially-reared B) wild type (n = 14), C) *lhfpl5b*^{vo35} (n = 18), D) *tomt*^{tk256c}(n = 13), E) *pcdh15a*^{th263b} (n = 13), and F) *cacna1da*^{tc323d} (n = 18) larvae at 4 dpf. Scale bar = 50 µm, applies to all images. G: Boxplots of qPCR results showing *pth2* expression in socially-reared mutants and siblings at 4 dpf. Ten larval heads were pooled per condition to make one biological replicate, and three biological replicates were used to generate the data. Two technical replicates of the qPCR experiment were conducted per biological replicate and averaged. One-way ANOVA to assess significance, ns = not significant.

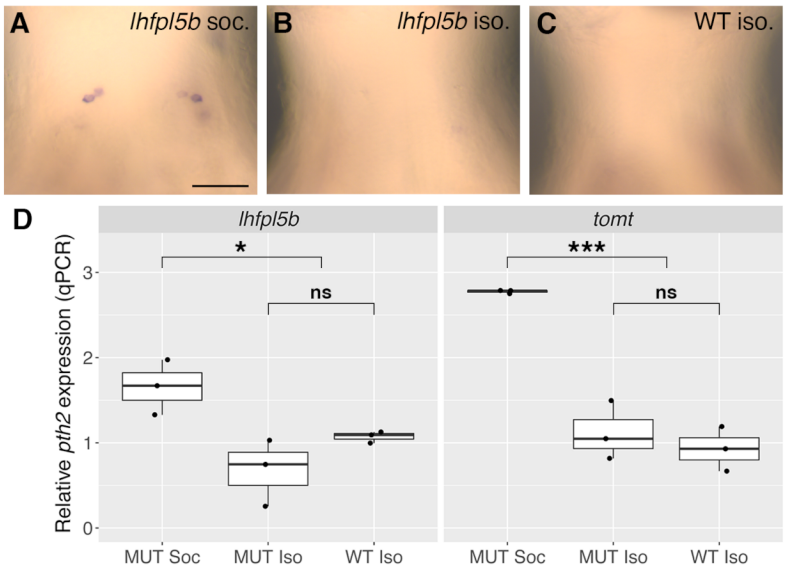

Fig. 3: Social isolation further reduces *pth2* expression in sensory hair cell mutants. (A-C) mRNA *in situ* hybridization showing representative examples of *pth2*-positive cells in 4 dpf A) socially-reared *lhfpl5b*^{vo35} mutants (n = 48), B) isolated wild type larvae (n = 50), and C) isolated *lhfpl5b*^{vo35} mutants (n = 40). Scale bar = 50 µm, applies to all images. D: Boxplots of qPCR results comparing *pth2* expression in socially-reared *lhfpl5b*^{vo35} and *tomt*^{tk256c} mutants relative to isolated mutant and wild type siblings at 4 dpf. Ten larval heads were pooled per condition to make one biological replicate, and three biological replicates were used to generate the data. Two technical replicates of the qPCR experiment were conducted per biological replicate and averaged. Two-way ANOVA to assess significance, *** = $p < 0.001$, * = $p < 0.05$, ns = not significant.

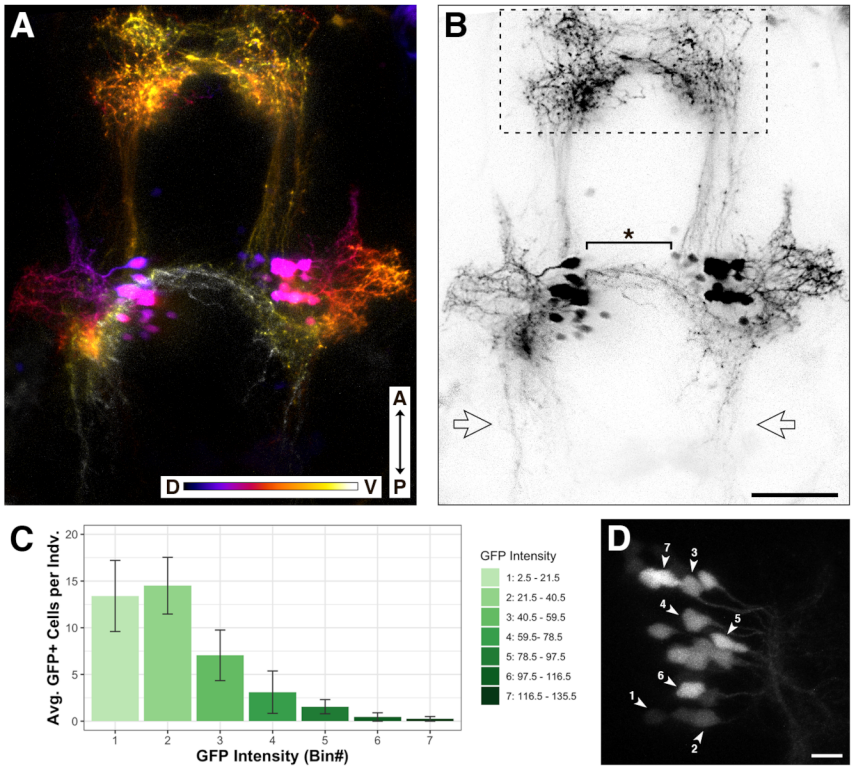

Fig. 4: Morphology of *pth2*-expressing cells using fluorescent reporters. A: Depth-encoded representation of the *Tg(pth2:TagRFP)unb3* transgenic line at 5 dpf. The anterior-posterior (A-P) axis and dorsal-ventral (D-V) depth color scale are indicated at the bottom. Image depth is 152 µm. B: Black and white version of the image in A. From the top: the dashed box indicates the anterior neuropil, the starred bracket highlights the ventral neurites that cross the midline, and the bilateral open arrows point to posterior neurites. Scale bar in B is 50 µm, applies to both images. See Movie S1 for a 3D rendering of the depth-encoded *pth2* transgene. C: Bar graph showing binned fluorescent intensity of GFP-positive cells (n = 20 larvae from 2 different clutches at 4 dpf). D: Zoomed-in image of one cell cluster exhibiting the full range of cell fluorescent intensity, labelled according to bins outlined in the associated bar graph. Image depth is 32 µm. Scale bar is 10 µm.

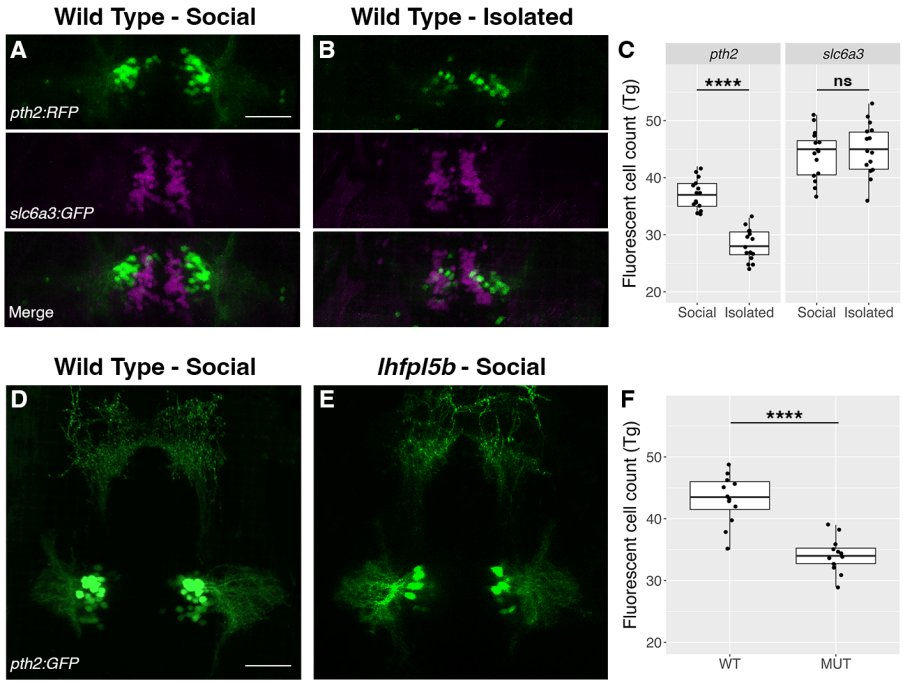

Fig. 5: The *pth2* transgenes respond to social context and lateral line input. (A-B) Representative images of *Tg*(*pth2:TagRFP)unb3* (false-colored green) and *Tg(slc6a3:EGFP)ot80* (false-colored magenta) transgenes in socially-reared and isolated larvae at 4 dpf. Merges of the two channels show the close proximity of the *pth2* and *slc6a3*-positive cell clusters. (C) Boxplots of *pth2* and *slc6a3* cell counts (n = 15 per condition). (D-E) Representative images of *Tg*(*pth2:EGFP)unb2* transgene expression in socially-reared wild type and lateral line mutant (*lhfpl5b*^{vo35}) larvae at 4 dpf. (F) Boxplots of GFP-positive cell counts in wild type (WT) and *lhfpl5b* mutant (MUT) siblings (n = 12 per condition). Scale bar is 50 µm. For both experiments, a one-tailed Welch's t-test was used to assess significance, **** = $p < 0.0001$, ns = not significant.

668 **SUPPLEMENTAL FIGURES AND LEGENDS:**

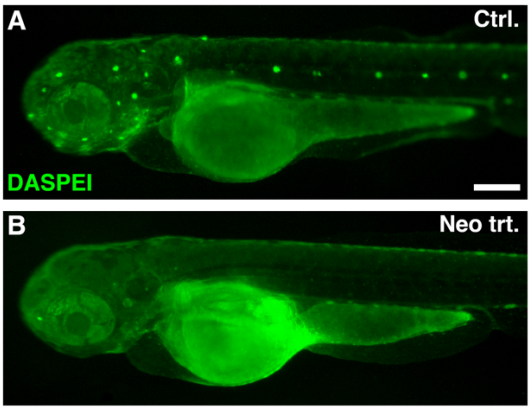

669

670 **Fig. S1: Vital dye staining of lateral line neuromasts in control and neomycin-treated larvae.**
671 Representative 3 dpf larvae from control (A) and neomycin-treated (B) groups stained with
672 DASPEI three hours following a 30-minute treatment with either 0 µM or 50 µM neomycin. Note
673 the near absence of punctate neuromast staining in B, indicating successful ablation of the lateral
674 line hair cells. Scale bar = 200 µm.

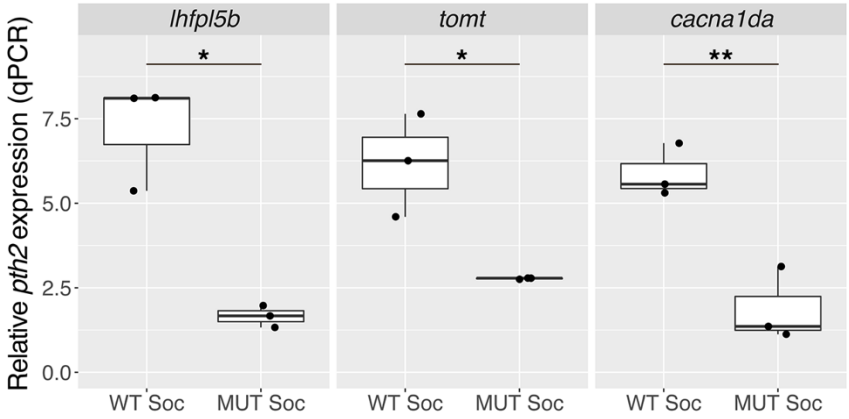

675

676 **Fig. S2: Boxplots of qPCR results showing *pth2* expression in socially-raised hair cell mutants**
677 **and wild type siblings at 4 dpf.** Ten larval heads were pooled per condition to make one
678 biological replicate, and three biological replicates were used to generate the data. Two technical
679 replicates of the qPCR experiment were conducted per biological replicate and averaged. A one-
680 tailed Welch's t-test was used to assess significance, * = $p < 0.05$, ** = $p < 0.01$.
681

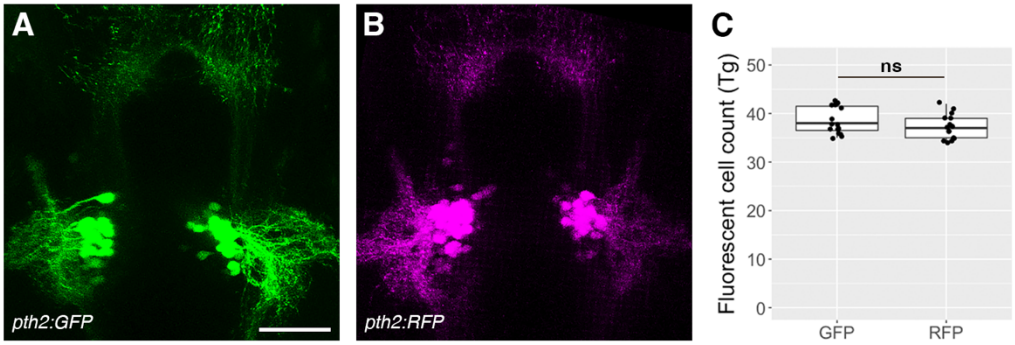

682

683 **Fig. S3: *Tg(pth2:EGFP)unb2* and *Tg(pth2:TagRFP)unb3* transgenes exhibit similar**
684 **morphology and number of cells.** (A-B) Representative images of socially-reared 4 dpf larva
685 possessing either the A) *Tg(pth2:EGFP)unb2* transgene (green) or B) *Tg(pth2:TagRFP)unb3*
686 transgene (magenta). (C) Boxplot of GFP and RFP cell counts (n = 15 larvae per condition). Scale
687 bar is 50 µm. A two-tailed Welch's t-test was used to assess significance, ns = not significant.

688

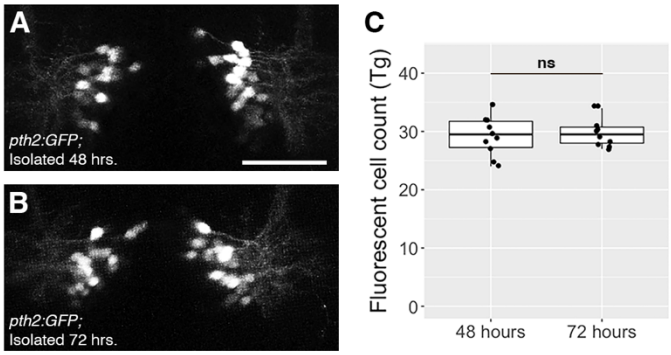

Fig. S4: Increasing the isolation period from 48 to 72 hours does not affect the number of GFP-positive cells in *pth2:GFP* transgenics. (A-B) Representative images of 4 dpf *Tg*(*pth2:EGFP)unb2* larva raised in isolation for A) 48 hours or B) 72 hours. (C) Boxplots of GFP-positive cell counts for *Tg(pth2:EGFP)* larvae raised in isolation for 48 or 72 hours (*n* = 10 per condition). Scale bar is 50 µm. A two-tailed Welch's t-test was used to assess significance, ns = not significant.

Movie S1: Related to Fig. 4A - Movie showing a 3D representation of cell morphology and neurite projections in a *Tg(pth2:TagRFP)unb3* zebrafish at 5 dpf. Projection depth is 152 µm.